Identification of carbon interstitials in electron-irradiated 6H-SiC by use of a ^{13}C enriched specimen

G. A. Evans and J. W. Steeds
Physics Department, University of Bristol, Bristol, United Kingdom

L. Ley and M. Hundhausen
Institut für Technische Physik, Universität Erlangen-Nürnberg, Erlangen, Germany

N. Schulze and G. Pensl
Institut für Angewandte Physik, Universität Erlangen-Nürnberg, Erlangen, Germany
(Received 16 July 2001; revised manuscript received 23 January 2002; published 19 July 2002)

Samples of 6H-SiC have been electron-irradiated with electron energies in the range 100–300 keV in a transmission electron microscope. After irradiation the samples were transferred to microscopic low-temperature photoluminescence spectrometers and excited by 325-nm, 488-nm, and 514.5-nm lasers. Optical centers were observed that had high-energy local modes and, when samples that had been enriched with ^{13}C during growth were examined, these local modes were split into triplets. The observations are interpreted as C-C dumb bells created from C interstitials generated during the irradiation process. This is the reported identification of self-interstitial atoms by photoluminescence in SiC.

DOI: 10.1103/PhysRevB.66.035204 PACS number(s): 61.72.Ji, 61.80.Fe, 78.55.Ap

I. INTRODUCTION

At present relatively little is known about self-interstitial atoms in SiC, but they are unavoidably involved in the processing of the material by ion implantation, oxidation, and annealing. Even in the case of elemental silicon there is still considerable uncertainty about their interstitial configurations, aggregations, motions, and involvement in diffusion processes.[1] In SiC, which can exist in several different polytypes, where both silicon and carbon interstitials may be created in a variety of different atomic environments, the situation is much more complex, and there are relatively few relevant theoretical calculations or definitive experimental results. It is therefore of particular interest to make the first direct observations related to the introduction of C interstitials and their migration during electron irradiation.

The technique that has facilitated this development is local-mode spectroscopy in low-temperature photoluminescence characterization of 6H-SiC. Local-mode spectroscopy, normally performed by infrared absorption or Raman spectroscopy, has proved a very fruitful means of obtaining information about point defects in semiconductors (see, for example, Ref. 2 and references therein). Since they have energies greater than the highest-energy longitudinal-optical modes of the bulk materials, they must be associated with lighter atoms than the host or greater local stiffness, or both. Much less common is the study of local modes associated with electronic transitions, though a considerable number of local modes have been studied by absorption or photoluminescence spectroscopy of electronic transitions in silicon[3] and in diamond.[4] As a general rule, local modes in both these materials have been deduced to be associated with in terstitial atoms, leading to an increase of lattice stiffness locally and hence higher vibronic frequencies. In the case of diamond, but not silicon, examples of threefold splitting of local modes have been recorded for mixed-isotope material and, when this occurred, the existence of a dumb-bell-shaped split self-interstitial configuration was inferred, although no detailed atomic model yet exists for any of these centers.[5] Calculations indicate that the stable interstitial in diamond is a $\langle 100 \rangle$ split dumb bell. Threefold splitting of local modes has also been found by the infrared spectroscopy of GaAs containing oxygen and here the atomic model advanced to explain the results is a Ga-O-Ga bridge associated with a V_{As}-O center with ^{69}Ga and ^{71}Ga isotopes.[6] Till now the only local modes (as distinct from gap modes) reported in SiC are associated with hydrogenated and deuterated samples[7] and these were rather short-lived under laser excitation. In this work we present the first evidence of luminescence centers in 6H-SiC that have triplet split local modes in ^{13}C-enriched material. Evidence will be presented that leads us to conclude that the local modes are caused by split carbon self-interstitials in the form of dumb bells.

In the past, in the absence of detailed calculations, simple formulas based on the vibrational modes of diatomic molecules have frequently been used to interpret local-mode data from crystalline solids.[4,6] We shall follow this approach in attempting to interpret our results.

Considerable effort has been directed at luminescence spectroscopy of irradiated SiC (Ref. 8) but, while a number of centers have been identified, on the whole atomic models are lacking. In the infrared region of the spectra, centers have been associated with neutral silicon vacancies.[9] The short-wavelength part of the specimen of irradiated 4H- and 6H-SiC, from 400 to 500 nm is much more complicated and not well understood. A recent careful study has identified a large number (34) of sharp zero-phonon lines (ZPL's) with associated vibronic structure in electron-irradiated 4H-SiC that can be grouped into twos, threes or fours by photoluminescence excitation spectroscopy performed at different temperatures.[10] These have been named the ''alphabet'' lines and the relevant region of the luminescence spectrum labeled

E_A by Egilsson *et al*., who draw attention to a related set of lines in the equivalent spectral region of 6H-SiC. The alphabet lines were deduced to arise from isoelectronic centers. By performing electron irradiations with electron energies below the silicon displacement energy we have shown that these alphabet lines are related to carbon displacements. We have also undertaken a careful correlation of results from these two polytypes that will be published independently. The centers to be reported here have not previously been described in the literature, although they exist in all the samples of 6H-SiC that we have examined (of which the samples forming the basis of this study were just a subset). The results that are presented here were extracted from several thousands of spectra generated from the irradiated samples. Details of the irradiation procedure are given elsewhere.[11]

In summary, circular regions of electron radiation damage of about 100 μm in diameter were created in the TEM and subsequently examined microscopically sometimes by area scans (each point in the scan generating a spectrum) and sometimes by line scans. Line scans were composed of between 20 and 200 spectra generated at equal intervals (typically 10 μm) along a line crossing the irradiated areas. Visual deconvolution of the data was performed subsequently to associate vibronic structure with prominent ZPL's. In the case of two-dimensional spectral arrays, wavelength-selected maps (sometimes referred to as spectra images in electron microscopic studies) were computer generated and spatial correlations established the relationships between vibronic structures and ZPL's. Although the spectra are admittedly quite complex the process of visual deconvolution (to be described) was remarkably effective, many of the subsidiary peaks varying greatly from one region to another, while the individual peaks of a particular vibronic structure remained in fixed relationships to each other and to the relevant ZPL.

II. EXPERIMENTAL DETAILS

The isotope-enriched 6H-SiC specimen investigated was grown by the modified Lely method using a mixture of 99% pure ^{13}C powder and natural silicon powder as source materials in a graphite crucible.[12] It was found to have approximately 30% of its carbon atoms replaced by ^{13}C as determined by Raman spectroscopy.[13] The 6H samples with natural abundance of C isotopes were both N-doped and Al-doped epilayers (at about 5×10^{15} cm^{-3}) obtained from Cree and high-quality *n*-type substrate material obtained from the Ioffe Institute, St Petersburg. Several room-temperature irradiations were performed, mainly at 300 kV but also down to 90 kV, with doses in the range from 5×10^{19} *e* cm^{-2} to 3×10^{20} *e* cm^{-2} in an ion-free Philips EM430 TEM. Altogether, more than 20 different irradiated areas were investigated. After irradiation the samples were transferred for photoluminescence studies to one of two Renishaw micro-Raman systems fitted with Oxford instruments microstat cryostages capable of operating down to temperatures of about 7 K. This was the temperature at which all the spectra presented in this paper were obtained. One of the Renishaw systems was operated at 325 nm using a He-Cd laser, the other was operated at 488 nm or 514.5 nm using an argon-ion laser. The spectra exhibited in this paper have small changes (±0.05 nm) in calibration over the period in which they were acquired but the energies quoted in this paper for local modes are accurate to ±0.2 meV. After initial investigation, some of the irradiated, naturally abundant, and isotope-enriched samples were annealed at a variety of temperatures up to 1300 °C and then reexamined by photoluminescence microscopy.

TABLE I. Zero-phonon line wavelengths and energies for natural abundance 6H-SiC samples.

ZPL	Wavelength (nm)	Energy (eV)
P_0	502.34	2.4674
Q_0	510.12	2.4298
R_0	510.79	2.4266
S_0	513.40	2.4142
T_0	514.57	2.4087
U_0	525.15	2.3602
V_0	521.5	2.377
Z_0	512.9	2.417

III. EXPERIMENTAL RESULTS

The irradiated specimens yielded a rich variety of spectral features with 325-nm, 488-nm, and 514.5-nm laser excitations. The majority of the features observed after 325-nm excitation were similar to those in the spectral region from 470 to 490 nm, named E_A by Egilsson *et al.*[10] and, in detail, closely related to the so-called alphabet lines of 4H-SiC. Slight shifts of the spectral lines occurred, similar to those reported by Sadowski *et al.*[14] for the N-bound exciton emission as a result of ^{13}C enrichment. We shall not be concerned with the alphabet lines here but analysis of our results is the subject of a separate publication.

In addition to these spectra a number of somewhat longer-wavelength lines were found, which have not been reported previously. They could all be observed with 488-nm excitation but only one of them, the 525-nm system, was also found with 325-nm excitation. Most of the spectra presented and analyzed here were obtained with 488-nm excitation. Table I gives the chief zero-phonon lines that occurred. We shall concentrate on P_0, Q_0, R_0, S_0, T_0, and U_0. They were generally observed in the *n*-type specimens in the as-irradiated condition but were normally absent from the *p*-type specimens (but there was one case when they were present in a *p*-type specimen). The spectra are, at first sight enormously complicated and we therefore start by describing how they were deconvoluted into their separate components by a different method that relies on the microscopic approach to optical spectroscopy that we have adopted. In view of this method, we start with a description of this procedure.

A typical low-temperature photoluminescence microscopy experiment involved generating spectra with the 488-nm laser in the spectral range 460–900 nm at equally spaced points across the irradiated region and extending well outside it. The result, called a line scan here, is a sequence of 20 and 200 individual spectra. More than 50 such line scans were

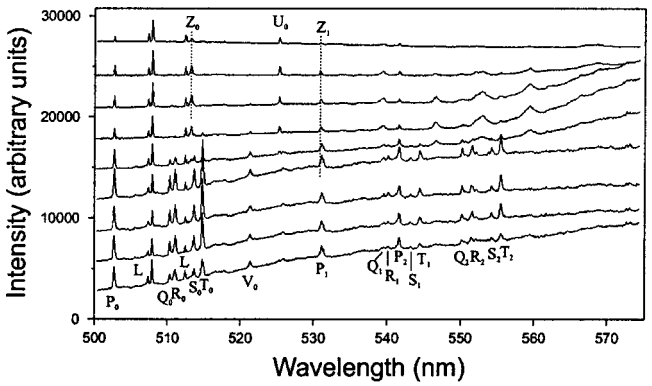

FIG. 1. Line scan across an electron-irradiated region of a sample of 6H-SiC with natural abundance of C. The spectra were excited with a 488-nm laser line with the specimen temperature ~10 K. The spacing between the points at which the spectra were recorded was 25 μm. Peaks labeled as L are Raman peaks. The zero-phonon lines discussed in this paper are P_0–U_0, with local modes P_1–T_1 and P_2–T_2. Note that the U_0 and Z_0 systems exist largely outside the irradiated region and that there is a small wavelength difference between peaks P_1 and Z_1.

studied in order to arrive at the conclusions reported here. As an example we show in Fig. 1 part of a line scan with spectra recorded at points spaced by 25 μm. The lower four spectra were recorded from the irradiated region itself, which was approximately 100 μm in diameter. The spectra above are from unirradiated regions. By examining these results it is possible to conclude that there are ten significant contributions. Those labeled L are the well-known Raman lines of 6H-SiC and are independent of irradiation. The centers V_0 and Z_0 were not central to this work. They were relatively easily distinguished from the other centers and had rather different properties. All the other centers, P_0, Q_0, R_0, S_0, T_0, and U_0 have associated vibronic structure that will be shown to account for the remainder of the spectral lines in the figure. As the centers P_0, Q_0, R_0, S_0, and T_0 were hardest to disentangle we start by discussing them. U_0, although rather different from these centers in some respects, had similar local-mode splitting and is therefore discussed towards the end of this section and is included in the tabulation of results.

To start with the most obvious conclusions, P_0 drops off very slowly outside the irradiated area while Q_0, R_0, S_0, T_0, and V_0 drop off more rapidly. By contrast, Z_0 and U_0 are negligible in the irradiated region but build up outside it. From other data, on different samples with different irradiations, the relative heights of P_0, Q_0, R_0, S_0, and T_0 change. In particular, some spectra are dominated by P_0, others have very strong T_0. However, certain subsets of peaks, such as P_0, P_1, and P_2 and T_0, T_1, and T_2 in Fig. 1, are found to appear in fixed intensity ratios. Measurement of the energies of the peaks gives almost the same energy difference of about 133 meV for (P_0-P_1) and (T_0-T_1) and around 179 meV for (P_0-P_2) and (T_0-T_2) (more accurate values appear in Table II). Having established these energy differences, similar connections can be found between Q_0, Q_1, and Q_2; R_0, R_1, and R_2; and S_0, S_1, and S_2. As the relative strengths of Q_0, R_0, and S_0 vary from one region to another and from one irradiation to another, the relative heights of Q_0, Q_1, and Q_2 stay approximately the same as do R_0, R_1, and R_2 and S_0, S_1, and S_2. On this basis, one can then attempt to identify some of the weaker spectral features (much more is made of this point later in the paper) so that the second-order peaks $2P_1$, $2Q_1$, $2R_1$, and P_1+P_2 can all be labeled. One additional experiment was performed to confirm the validity of the above assignments. As the ZPL of the T_0 system occurs at a wavelength of approximately 514.5-nm in the natural carbon sample, an attempt was made to excite this system resonantly by adjusting the argon-ion laser to 514.5 nm emission. When this was carried out the resulting spectra revealed strong enhancement of the T_1 and T_2 local modes as well as the sum modes corresponding to T_1+T_2 and $2T_2$ (Fig. 2) in agreement with the peak analysis that has been described. The existence of this (T_1+T_2) sum peak and the (P_1+P_2) sum peak referred above confirm that the two local modes summed come from a common ZPL. The energy of the sum peak agrees with the sum of the two energies to within 0.1 meV.

As 133 meV and 179 meV are greater than the energy of the most energetic longitudinal-optic phonons (120 meV) in 6H-SiC, we conclude that these are local modes. That being the case, it follows that spectra related to these local modes should exhibit the characteristics that are well known for such modes. These characteristics are concerned with the relative intensities, energy separations, and linewidths of

TABLE II. Details of the local modes of the zero-phonon lines (ZPL's) P_0–U_0. S_n is the value of the Huang-Rhys factor for the nth local mode and w_n/w_0 is the ratio of width of the nth first-order local mode to that of the ZPL. w' is the width of the second-order local mode. * indicates resonant excitation; note the higher accuracy achieved and the additional data. I_{2LM}/I_{LM} is the ratio of the intensity of the second-order local mode to that of the first-order local mode.

	LM_1 (meV)	w_1/w_0	S_1	LM_2 (meV)	$(2LM_2-LM_2)$ (meV)	w_2/w_0	w'/w_2	S_2	I_{2LM}/I_{LM}
P	133.2	1.91±0.14	0.43±0.06	179.3	176.8	1.37±0.06		0.79±0.15	
Q	132.7	1.61±0.23	0.30±0.07	178.1	175.6	1.28±0.04		0.63±0.09	
R	132.3	1.24±0.05	0.22±0.01	180.2	177.6	1.37±0.15		0.69±0.15	
S	133.0	1.60±0.23	0.39±0.14	178.9		1.35±0.19		0.58±0.13	
T	132.9	1.60±0.14	0.34±0.07	178.4	176.2	1.34±0.07	2.18±0.06*	0.71±0.09	0.35±0.07
U				246.6	245.1	1.59±0.07	1.61±0.13	0.96±0.11	0.21±0.03

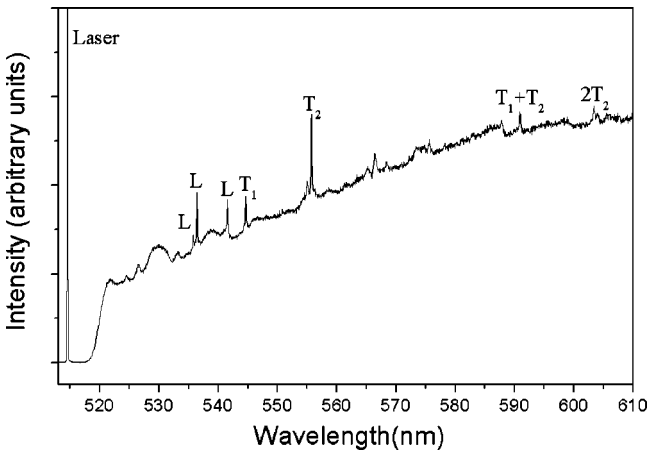

FIG. 2. Resonant enhancement of the T system by use of 514.5-nm laser excitation with the sample at ~ 10 K. Peaks labeled L are Raman peaks. A sum mode (T_1+T_2) and a second-order local mode $(2T_2)$ are marked. This result is a significant step towards the deconvolution of the spectra under investigation.

successive orders of local modes.[15] The rate of drop-off of intensity of successive peaks is measured by the Huang-Rhys factor (S). If the ZPL has intensity I_0 at frequency ω_0 and the first-order local mode has intensity I_1 at frequency ω_1 then S is given by

$$S=\left(\frac{\omega_0}{\omega_1}\right)^3\frac{I_1}{I_0}. \tag{1}$$

Anharmonic effects cause a reduction in the energy separation of successive orders of local mode that, to a first approximation, is linearly related to the order and an increase in linewidth (w) that is also linearly related to the order of the local mode. The data in Table II illustrate that, as far as can be determined from only two orders of local mode at most, the systems based on ZPL's P_0–U_0 are consistent with these characteristics.

Having thus explained the methodology on which this paper is based we now concentrate on the ZPL's P_0–U_0. It has not been possible to obtain the complete spectrum of each of the systems associated with these ZPL's uncontaminated by others, but their relative strengths were found to vary from sample to sample, from one region to another and with annealing. In particular, although all of the centers were found in the as-irradiated condition, there was some difference between the annealing behavior of n- and p-type samples. In p-type samples the P_0 center was greatly reduced in intensity after a 900 °C anneal and the centers Q_0–T_0 had gone completely. In n-type samples the intensities of the P_0–T_0 centers were unaffected by annealing to the same temperature. Both n- and p-type samples exhibited considerable growth of U_0 (and Z_0) luminescence after annealing to 900 °C and these centers were stable up to 1300 °C, the highest annealing temperature used. Accompanying this growth of U_0 intensity there was a marked change in its distribution, with the maximum intensity occurring at the center of the irradiated region whereas it had been confined to regions outside the irradiated region itself, in the as-irradiated state, if present at all. When a p-type sample was annealed to 1300 °C the U_0 luminescence became very strong within the irradiated region but dropped off rapidly outside.

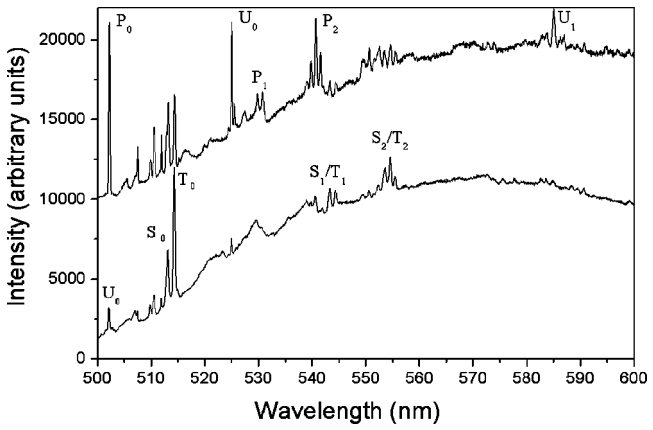

FIG. 3. Two spectra from the isotope-enhanced specimen of electron-irradiated 6H-SiC with very different relative intensities of the P_0–U_0 zero-phonon lines. The spectra were recorded at ~ 10 K using 488-nm excitation.

A parallel set of experiments was performed on the isotope-enriched sample and Fig. 3 shows two spectra obtained from different samples where the relative strengths of the ZPL's P_0–T_0 varied considerably. Careful examination of these results, to be described, leads to the conclusion that the 133-meV local mode of each of P_0, Q_0, R_0, S_0, and T_0 splits into two approximately equal components in the isotope-enhanced specimens while the 179-meV local mode splits into three with intensity ratios of approximately 1:2:1. First, we consider the lower of the two spectra in Fig. 3. The higher-energy peak of the doublet in the region marked S_1/T_1 is at approximately 133 meV from T_0; the highest-energy peak of the complex in the region marked S_2/T_2 is at approximately 179 meV from T_0. By peak fitting the spectra in these regions, and also in the other regions indicated in Fig. 4, the peak energies were determined and interpreted as originating from ZPL's Q_0–T_0 as shown in the figure. A similar procedure was also carried out for the upper spectrum

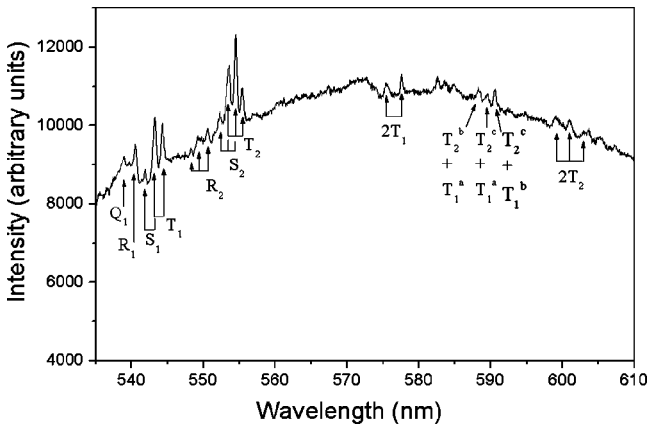

FIG. 4. Assignments of the spectral details in the region 530–610 nm of the lower spectrum in Fig. 3 to local modes of Q_0, R_0, S_0, and T_0.

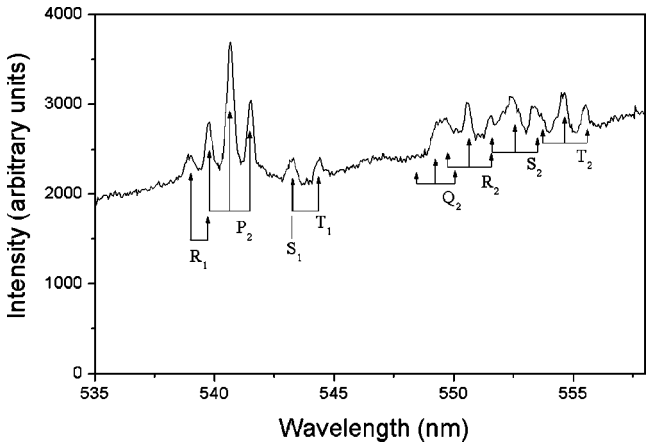

FIG. 5. Assignments of the spectral details in the region 535–558 nm of the upper spectrum in Fig. 3 to local modes of Q_0, R_0, S_0, and T_0.

in Fig. 3 where the P_0 ZPL was particularly strong. Figure 5 shows the relationships to the ZPL's P_0–T_0, which were deduced as a result. A detail of this fitting procedure is shown in Fig. 6 from the most complex spectral region, that of S_2/T_2 in the upper spectrum of Fig. 3. It can be seen that this is well fitted by triplets of lines in the ratio of approximately 1:2:1 as indicated in Fig. 5. The single exception is the highest-energy line of the S_2 triplet, which is considerably more intense than the two lower-energy lines of the triplet. We believe that this discrepancy is explained by an additional unrelated peak at the same wavelength. As a result of these peak-fitting procedures the energies of the various local modes were deduced and they are given in Tables III and IV.

Although the spectra obtained were too complicated to yield accurate values for the relative intensities of the lines in the doublets and triplets, approximate values can be derived. For example, the doublet marked P_1 in the upper spectrum of Fig. 3 has two lines of approximately equal intensity. Our

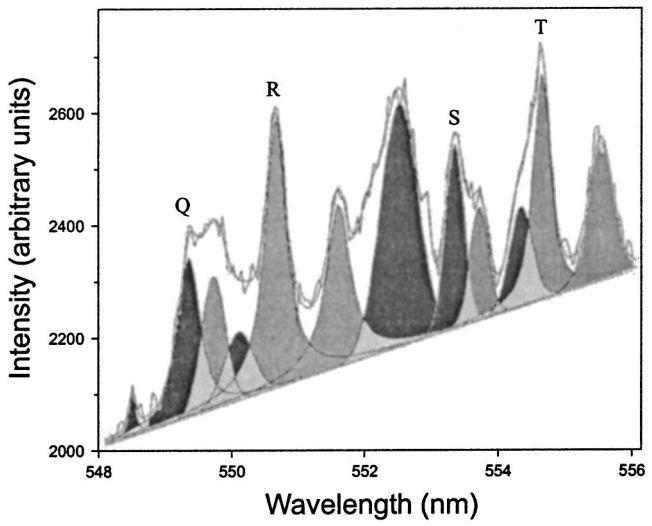

FIG. 6. Peak fitting for the local-mode peaks in the region Q_2–T_2 of Fig. 5.

TABLE III. Details of the lower-energy local modes of zero-phonon lines P_0–T_0 in the isotope-enriched sample.

	Iso (13) (meV)	Iso (12) (meV)	Natural (meV)	Ratio
P	128.67	133.0	133.2	1.034
Q	128.45		132.7	1.033
R	128.03		132.3	1.033
S	128.6		133.0	1.034
T	128.41	132.94	132.9	1.035

peak fitting of the regions S_1/T_1 of the spectra (see Figs. 3 and 4) was also in agreement with this conclusion, the shorter-wavelength peak being slightly less intense than the longer-wavelength peak. Peak fitting of the regions S_2/T_2 of the spectra led to the conclusion that the triplet peaks were approximately in the ratio 1:2:1 (see, for example, Fig. 6) but with the shortest-wavelength peak of slightly lower intensity (by about 10%) than the longest-wavelength peak in the triplet.

Whereas the ZPL's labeled P_0, Q_0, R_0, S_0, and T_0 have rather similar values for their local modes, U_0 exhibits quite different behavior. Since the annealing conditions for optimizing the U_0 system were rather different from those for P_0–T_0 emission, there was no difficulty in separating out the features of its spectrum from the P_0–T_0 systems. However, the system associated with the Z_0 ZPL tended to increase on annealing, together with the U_0 system (Fig. 7). However, in some regions Z_0 could be found with virtually no U_0 and hence its associated peaks Z_a–Z_d could be identified easily (Fig. 8). The U_0 spectrum has a well-defined vibronic structure (underlined in Fig. 7) with a very strong local mode U_1 at 246.6 meV from U_0 and a second-order local mode $2U_1$. There is apparently no local mode of lower energy than U_1. The vibronic structure of the system (underlined) is repeated as sum peaks (also underlined) to the local mode U_1 but the Z_a–Z_d peaks are not, as anticipated. The second-order local mode occurs at 245.1 meV from the first-order local mode.

In the case of the electron-irradiated isotope-enriched specimen, triplet splitting of the 246.6-meV local mode was observed (Fig. 9). Values for the local-mode energies measured are given in Table IV. It is notable that, in this case, the intensity of the shortest-wavelength local mode is significantly higher than that of the longest-wavelength local mode. No splitting of spectral lines was observed for the Z_0 system.

The involvement of carbon atoms in these optical centers is established not only by the isotope-dependent shifts but also by the electron energies at which the centers have been created. In previous work it has been established that silicon vacancies are not created at electron energies of 225 keV and below in 4H-SiC.[8] Similar results have also been obtained in the case of 6H-SiC (to be published independently) but the critical energy for Si displacement is around 200 keV. However, the P_0–T_0 centers have been found in samples irradiated at electron energies of 170 keV, below the silicon displacement threshold.

The question arises whether the centers P_0–T_0 are all independent of each other. The main evidence that they are

TABLE IV. Details of the higher-energy local modes of zero-phonon lines P_0–T_0 and of U_0 in the isotope-enriched sample.

	Iso (13) (meV)	Iso (12/13) (meV)	Iso (12) (meV)	Natural (meV)	Ratios 12−12/12−13	Ratios 12−12/13−13
P	172.2±0.1	175.9±0.1	179.5±0.1	179.3	1.020	1.042
Q	170.4±0.5	174.6±0.2	178.1±0.1	178.1	1.020	1.045
R	172.0±0.7	176.0±0.4	179.7±0.7	180.2	1.021	1.045
S	171.7±0.2	175.8±0.7	179.0±0.8	178.9	1.018	1.043
T	171.4±0.15	175.0±.05	178.7±.05	178.4	1.021	1.043
U	237.4	242.1	246.6	246.6	1.019	1.039

comes from the fact that, although each of these five zero lines were generally present in the as-irradiated condition, their relative strengths varied considerably between samples. The most frequently encountered situation was where the intensity of Q_0 was considerably less than that of R_0 and that of S_0 considerably less than T_0. However, spectra were recorded with S_0 but virtually no T_0 and with Q_0 and R_0 at approximately the same intensity. Spectra were recorded where the intensity of P_0 was much greater than Q_0–T_0 and others had P_0 much less than Q_0–T_0.

IV. DISCUSSION OF RESULTS

One of the chief challenges confronting this investigation was that of splitting up the complex spectra observed into separate components. One means of achieving this was by spatial correlation, another was by measuring the relative intensities of spectral lines in different spectra. A third means was by resonant excitation of a specific ZPL (Fig. 2), fourth one was measurement of energies and linewidths of local modes, and a fifth was by the identification of sum modes, on the basis of energy addition. A sixth was by the use of samples with C-isotope enhancement. Another challenge was that of relating the individual optical centers to atomic models. For this exercise the C-isotope enhanced material was invaluable. The splitting of local modes indicated how many C atoms are involved in a particular mode of vibration. The energies of the splittings observed could be directly related to the change of C mass.

The shifts of the ZPL's of each of the optical centers studied here was to shorten wavelength in the ^{13}C-isotope-enhanced material. These shifts were small, in the range 1–2 meV, comparable with, but slightly smaller than, C-isotope-related shifts of ZPL's of interstitial-related centers in diamond.[16] There are several contributions to these increases of energy, including the decrease in lattice volume on changing from ^{12}C to ^{13}C and the anharmonicity of vibrations centered on the defect.[12] We shall not pursue the interpretation of the shifts that were recorded in this work.

The main interest of this work is the properties of the local modes that have been reported. The number of components that a local mode splits into in the case of the isotope-enriched specimen indicates the number of carbon atoms involved. Thus the twofold splitting of the 133-meV modes indicates the involvement of one carbon atom and the threefold splitting of the 179-meV and 247-meV local modes indicates the involvement of two carbon atoms.

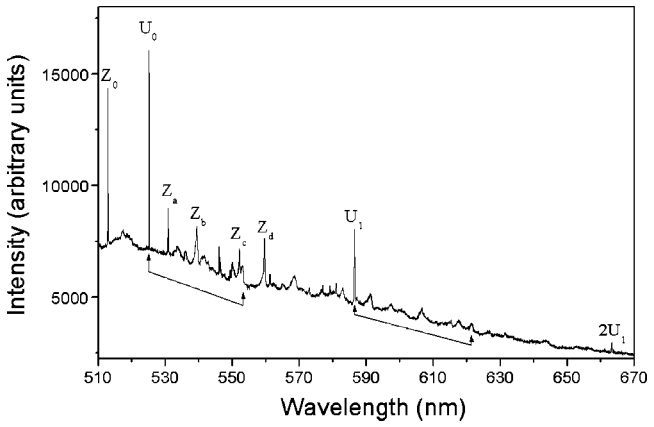

FIG. 7. Typical spectrum obtained from a 6H-SiC specimen, with natural C abundance, annealed at high temperature (900–1100 °C) after electron irradiation. Two spectra, with ZPL's Z_0 and U_0, are superimposed. Subsidiary peaks of the Z_0 ZPL are labeled Z_a–Z_d (see Fig. 8). First- and second-order local modes of the U_0 ZPL are marked. The regions underlined are the vibronic structures, up to the bulk phonon cutoff, of the ZPL and the first-order local mode. Spectrum is recorded at ~10 K using 488-nm excitation.

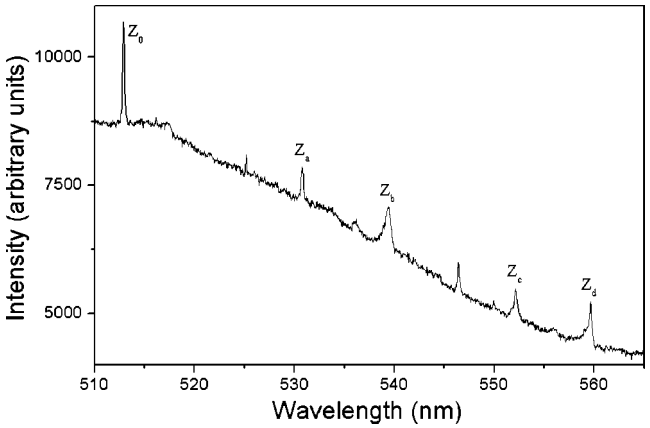

FIG. 8. Z photoluminescence system with only very small U_0 intensity at 525 nm. Spectrum is recorded at ~10 K using 488-nm excitation.

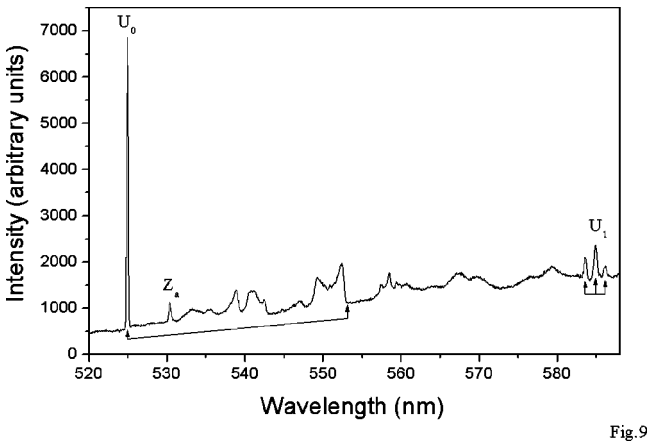

FIG. 9. *U* luminescence system obtained from the isotope-enhanced sample after electron irradiation (488-nm excitation, ~10 K). Weak contamination of this spectrum with *Z* luminescence is indicated. Note the triplet splitting of the local mode U_1 and the vibronic region (underlined) of U_0 terminated at an energy corresponding to the highest-energy bulk longitudinal-optic phonons.

In order to arrive at conclusions about the above configurations of the optical centers giving rise to these local modes it would be helpful to have detailed calculations for local-mode energies. The existence of the local modes indicates the involvement of interstitial atoms rather than vacancies. The high energy of the local modes indicates the involvement of light atoms and increased stiffnesses. This conclusion is consistent with the association of the optical systems with carbon atoms, on account of the low electron energies at which the centers are produced. Calculations for self-interstitials in SiC have been published only for the cubic polytype. It was found that C-C split interstitials in both ⟨100⟩ and ⟨110⟩ orientations were stable, but that the ⟨100⟩ orientation had a much lower energy of formation.[17] Recent calculations for the doubly positively charged ⟨100⟩ split C-interstitial in 3C-SiC gave a single local vibrational mode with an energy of 219.4 meV.[18] In the same work other interstitial complexes in 3C-SiC were investigated including a ⟨100⟩ oriented C-C dumb bell with the carbon atoms replacing a Si site. This defect was found to have five local modes, the highest energy varying from 176.7 to 179.4 meV depending on the charge state (from $++$ to $--$). Two of the other local modes were calculated as 135.2 meV in the doubly negative charge state and another varied from 126.7 to 128.5 meV as the charge state changed from $++$ to 0. Although these energies are close to those observed here, detailed consideration indicates that agreement between these models and our experiments has not yet been achieved. First, we do not have centers with either just one, or alternatively, with five local modes. Second, the ⟨100⟩ C-C dumb bell occupying a Si site is shown[18] to be a reasonable model for the D_{II} center. This not only has a ZPL at a shorter wavelength in 6H-SiC but it is chiefly created by ion implantation with subsequent annealing to about 1000 °C. Our own results were created by low-voltage electron irradiation, and the centers discussed here were created with electron energies (150 keV) well below the Si displacement threshold[8] and could be observed without annealing. D_{II} luminescence was not observed.

As these are the only relevant calculations, we have to resort to molecular models in order to analyze our results in more detail. Justification for this approach can be found in its success in previous works for centers in diamond[19] and GaAs[6] and also from a comparison of results for the local-mode energies calculated by Breuer and Briddon[20] with those for a C-C diatomic molecule. Their numbers for ^{13}C-^{13}C, ^{12}C-^{13}C, and ^{12}C-^{12}C isotope pairs agree quite accurately with values deduced from the square root of the relevant mass ratios. We have, therefore, included in Table IV values for the ratios of the local-mode energies. These ratios should be compared with 1.020 for the reduced mass ratio of equal proportions of ^{13}C and ^{12}C to ^{13}C and 1.041 for the ^{13}C to ^{12}C mass ratio. The close agreement with experiment clearly indicates that the higher-energy local modes of optical centers P_0–T_0 are caused by C-C split-interstitial dumb bells.

Although the intensity ratios of the two lines of the ~133-meV doublet and the outer lines of the 179-meV triplet were not very accurately determined, the slightly smaller intensity of the shorter-wavelength lines indicates a smaller concentration of ^{13}C than of ^{12}C. Using intensity values from the P_2, R_2, and T_2 triplet splittings for a sample with a composition of $^{13}C_x$ $^{12}C_{1-x}$ we expect the outermost intensity ratios to be x^2:$(1-x)^2$. Our results indicate $x \approx 0.47$, a value considerably higher than that derived from the Raman experiments.[13] The samples were shown in Ref. 13 to have an x variation with depth, but even so our value is significantly higher than the highest value determined by the earlier experiments. We lack an adequate explanation for this discrepancy at present.

It has been established that the split self-interstitial in diamond takes the form of a dumb bell aligned along ⟨100⟩ but in silicon the ⟨110⟩ orientation has been found to be more stable.[20,21] One possible explanation of the five centers could be that the A_0 center is aligned in 6H-SiC along the directions equivalent to ⟨100⟩ in the cubic lattice and the other four centers are produced by dumb bells along directions equivalent to ⟨110⟩ in the cubic lattice. Three of these lie in the basal plane, three are at approximately 60° to those in the basal plane. Pseudocubic or pseudohexagonal environments[22] could give rise to slight splitting of the energies of the centers. Thus Q_0 and R_0 might correspond to one of the two different ⟨110⟩ orientations and S_0 and T_0 to the other. The fact that the electron beam was incident along [0001] might indicate that S_0 and T_0, which were always somewhat more intense than Q_0 and R_0, correspond to the inclined ⟨110⟩ directions and Q_0 and R_0 to directions in the basal plane.

In the cubic ⟨100⟩ and ⟨110⟩ split-interstitial models, Fig. 10, each of the carbon atoms is involved in a Si-C-Si bond.[17] In the case of the ⟨100⟩ split interstitial in diamond the semi-angle between the bonds is calculated as 70.5°.[20] Vibrational modes involving this particular bond (β in diagram) have only one C atom and might therefore account for the 133-meV local modes that split into two approximately equal

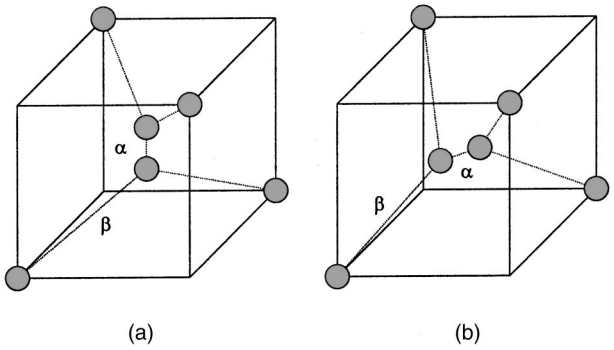

FIG. 10. Atomic models for (a) the ⟨100⟩, and (b) the ⟨110⟩ C split-interstitial dumb bells.

components in the isotope-enhanced specimen (the existence of just two components implies that any defect-related, symmetry-breaking distortions are small). As a test of this hypothesis we have investigated the modes of a hypothetical Si-C-Si molecule according to the analysis of Herzberg[23] and its use in the interpretation of the Ga-O-Ga bridge.[6] For a symmetrical XY_2 molecule where the bond angle is 2θ there are two symmetrical and one antisymmetrical vibrational modes. For the antisymmetrical mode the vibrational frequency has an analytical form expressed by

$$\nu \propto \sqrt{\frac{1}{m_y}+\frac{2\sin^2\theta}{m_x}}. \tag{2}$$

This was the expression used in by Schneider *et al.*[6] to interpret their results. Substituting values into this expression using an approximate value $\theta=70°$ we obtain a ν_{12}/ν_{13} ratio of 1.033 somewhat lower than that for the C-C bond and quite close to the relevant values in Table II. While this qualitative approach should not be taken too seriously, it does support the conclusion that the P_0–T_0 centers are caused by C-C split interstitials.

The next result to discuss is the triplet splitting of the 247-meV local mode of U_0. The threefold splitting again indicates the involvement of two carbon atoms in the center but, in this case, the ratio of the local-mode energies is not in good agreement with the ratio of the square root of the masses of ^{13}C and ^{12}C. The remarkably high energy of the local modes of the U_0 center, more than twice the highest energy of the longitudinal-optic modes of 6H-SiC, has also to be explained. Resorting, once again, to comparison with the vibrational modes of molecules the most likely candidate for such a high energy is the involvement of hydrogen in the center. This conclusion is supported by recent theoretical work on the stretching vibrational modes of H in SiC where energies comparable to those found here as well as much higher energies are reported.[24] Supporting evidence for this conclusion comes from the observed spatial distribution of these centers. When they occurred in the as-irradiated condition, which was not always the case, they were restricted to the periphery, outside the actual area of irradiation. On annealing above 1000 °C the U_0 center became quite strong and was concentrated at the center of the irradiated region. H atoms, being light, would be displaced from the irradiated region by the incident electron beam but would diffuse back again on annealing. It is also worth pointing out that our results indicate that the interstitial atoms created during the irradiation process migrate significant distances outside the actual region of irradiation. After high doses of the order of $3\times10^{20}e\ \mathrm{cm}^{-2}$ these migration distances are several tens of micrometers. This result is similar to that previously reported in diamond after similar electron doses[25] and is the subject of an independent publication.

The absence of P_0–T_0 luminescence from spectra generated by above band-gap excitation probably explains why these centers have not previously been reported in earlier work. The implication is that the centers undergo a change of charge state either by ionization or by the availability of free carriers. In view of the loss of Q_0–T_0 luminescence and the reduction of P_0 intensity in *p*-type material after 900 °C annealings, it is likely that this change of charge state is induced by the presence of free holes in the material. On irradiation, the damaged areas of *p*-type material experience a shift of Fermi level towards the middle of the band gap, eliminating or reducing the generation of holes under 488-nm excitation, but on annealing, the damage is reduced (many of the alphabet lines are eliminated) and holes are once again generated.

V. SUMMARY

We have presented results of a different method for generating and investigating point defects in semiconductors that is able to discriminate between carbon and silicon displacements in 6H-SiC. The properties of this method have been exploited to deconvolute complex low-temperature photoluminescence spectra into individual ZPL's and their associated local modes. As a result, five closely related new centers have been discovered each with local-mode energies of approximately 133 meV and 179 meV. Observations of local-mode splitting in a sample with its carbon component enriched by ^{13}C substitution have allowed us to identify optical centers associated with C-C split interstitial dumb bells in 6H-SiC. The 133-meV modes are identified as Si-C-Si stretching modes and the 179-meV modes as C-C stretching modes. The implication of these results for future studies of diffusion, accumulation, and loss of carbon interstitials in 6H-SiC are significant. Possible reasons for the existence of five different but closely related centers have been advanced.

In addition, one further new optical center has been identified. This differs considerably from the other five in having a much higher local-mode energy of 247 meV. Threefold splitting of this mode in the isotope-enhanced sample indicates that it also involves two carbon atoms but, in this case, these are not in the form of a C-C dumb bell and there is no equivalent of the Si-C-Si stretching mode.

Under the irradiation conditions used in these experiments interstitial carbon atoms were found to migrate several tens of micrometers outside the electron-irradiation region itself.

ACKNOWLEDGMENT

We wish to thank Dr. J. M. Hayes for critical reading of the manuscript.

[1] S.K. Estreicher, M. Gharaibeh, P.A. Fedders, and P. Ordejon, Phys. Rev. Lett. **86**, 1247 (2001); U. Gösele, Nature (London) **408**, 38 (2000).
[2] M.D. McCluskey, J. Appl. Phys. **87**, 3593 (2000).
[3] G. Davies, Phys. Rep. **176**, 83 (1989).
[4] A.T. Collins and S.C. Lawson, J. Phys.: Condens. Matter **1**, 6929 (1989).
[5] J.W. Steeds, T.J. Davis, S.J. Charles, J.M. Hayes, and J.E. Butler, Diamond Relat. Mater. **8**, 1847 (1999).
[6] J. Schneider, B. Dischler, H. Seelewind, P.M. Mooney, J. Lagowski, M. Matsui, D.R. Beard, and R.C. Newman, Appl. Phys. Lett. **54**, 1442 (1989).
[7] W.J. Choyke and L. Patrick, Phys. Rev. B **9**, 3214 (1974).
[8] W.J. Choyke, Inst. Phys. Conf. Ser. **31**, 58 (1977); J.W. Steeds, F. Carosella, G.A. Evans, M.M. Ismail, L.R. Danks, and W. Voegeli, Mater. Sci. Forum **353-356**, 381 (2001).
[9] M. Wagner, B. Magnusson, W.M. Chen, E. Janzén, E. Sörman, C. Hallin, and J.L. Lindström, Phys. Rev. B **62**, 16 555 (2000).
[10] T. Egilsson, A. Henry, I.G. Ivanov, J.L. Lindström, and E. Janzén, Phys. Rev. B **59**, 8008 (1999).
[11] J.W. Steeds, S.J. Charles, J. Davies, and I. Griffin, Diamond Relat. Mater. **9**, 397 (2000).
[12] N. Schulze, D.L. Barett, and G. Pensl, Appl. Phys. Lett. **72**, 1632 (1998).
[13] S. Rohmfeld, M. Hundhausen, L. Ley, N. Schulze, and G. Pensl, Phys. Rev. Lett. **86**, 826 (2001).
[14] H. Sadowski, N. Schulze, T. Frank, M. Laube, G. Pensl, and R. Helbig, Mater. Sci. Forum **353-356**, 401 (2001).
[15] A.T. Collins and P.M. Spear, J. Phys. C **19**, 6845 (1986).
[16] A.T. Collins, G. Davies, H. Kanda, and G.S. Woods, J. Phys. C **21**, 1363 (1988).
[17] M. Bockstedte and O. Pankratov, Mater. Sci. Forum **338-342**, 949 (2000).
[18] A. Mattausch, M. Bockstedte, and O. Pankratov, Physica B **308**, 656 (2001); M. Bockstedte, A. Mattausch, and O. Pankratov, Mater. Sci. Forum **353**–**356**, 447 (2001).
[19] G. Davies, I. Kiflawi, G. Sittas, and H. Kanda, J. Phys.: Condens. Matter **9**, 3871 (1997).
[20] S.J. Breuer and P.R. Briddon, Phys. Rev. B **51**, 6984 (1995).
[21] D.J. Chadi, Phys. Rev. B **46**, 9400 (1992).
[22] L. Patrick, Phys. Rev. **127**, 1878 (1962).
[23] G. Herzberg, *Infrared and Raman Spectra of Polyatomic Molecules* (Van Nostrand, New York, 1964).
[24] B. Aradi, A. Gali, P. Deak, J.E. Lowther, N.T. Son, E. Janzén, and W.J. Choyke, Phys. Rev. B **63**, 245202 (2001).
[25] J.W. Steeds, S. Charles, T.J. Davis, A. Gilmore, J. Hayes, C.D.O. Pickard, and J.E. Butler, Diamond Relat. Mater. **8**, 94 (1999).